Contribution from the Department of Chemistry,
The University of Western Ontario, London, Ontario, Canada N6A 5B7

Absorption and Magnetic Circular Dichroism Spectroscopy of Metal- and Ring-Oxidized Porphyrins. Spectral Characteristics of the One- and Two-Electron Oxidation Products of Cobalt Octaethylporphyrin

Zbigniew Gasyna† and Martin J. Stillman*

Received February 27, 1990

One- and two-electron oxidation products of cobalt(II) octaethylporphyrin, $Co^{II}OEP(-2)$, have been characterized by optical absorption and MCD spectroscopy. One-electron oxidation leads either to the metal-oxidized complex, $[Co^{III}OEP(-2)]X$, or to the porphyrin-ring-oxidized species, $[Co^{II}OEP(-1)]^{\bullet+}X^-$, depending on the ligand, X^-, that is present. With $X^- = Cl^-$, Br^-, and $SbCl_6^-$, metal oxidation is observed, while with $X^- = ClO_4^-$, ring oxidation takes place. The spectral properties of the π-cation-radical species, $[Co^{III}OEP(-1)]^{\bullet 2+}(X^-)_2$, that are formed following the two-electron oxidation of $Co^{II}OEP(-2)$ vary significantly for the Cl^-, Br^-, ClO_4^-, and $SbCl_6^-$ counterions. The differences between the spectral properties of a range of oxidized complexes have been investigated by using deconvolution analysis of the absorption and MCD spectra to provide quantitative information about the energies of bands that contribute to the observed spectral envelope. The relationship between the spectroscopic data and the two possible radical ground states, $^2A_{1u}$ or $^2A_{2u}$, that are accessible to the porphyrin π-cation-radical species is discussed. The patterns of bands that are characteristic of the $^2A_{1u}$ or the $^2A_{2u}$ ground states for the π-cation-radical species are described by comparing the absorption and MCD spectral data formed by ring oxidation of zinc tetraphenylporphyrin and magnesium octaethylporphyrin to the π-cation-radical complexes $[ZnTPP(-1)]^{\bullet+}$ and $[MgOEP(-1)]^{\bullet+}$ with the data from the CoOEP complexes. The MCD spectral data show that π-ring oxidation always leads to the appearance of characteristic spectral features in the visible region that can be used as a fingerprint for ring oxidation compared with metal-based oxidation. This spectral envelope is observed for both the Co(II) and Co(III) π-cation-radical complexes.

Introduction

Metalloporphyrin complexes can be oxidized chemically, electrochemically, or photochemically to form either metal- or porphyrin-ring-centered oxidized products.[1-5] We have previously used MCD spectroscopy to aid in the discrimination between these types of products for both porphyrins and phthalocyanines.[4-6] Oxidation of $Co^{II}OEP(-2)$[7] by electrochemical[8] and chemical[9] methods leads to a variety of one- and two-electron oxidized products. Significantly, one-electron oxidation of $Co^{II}OEP(-2)$ can result in either metal-oxidized[10] or porphyrin-ring-oxidized[11] species. Two-electron oxidation forms the $[Co^{III}OEP(-1)]^{\bullet 2+}$ species.[4] MCD spectra provide a precise assignment criterion for the states involved in porphyrin absorption spectra and, therefore, a method of identifying the electronic configuration on the chromophore.

Oxidation of metalloporphyrin[1-4] and metallophthalocyanine[5,12] π-ring systems significantly alters the optical absorption spectrum. For porphyrins, the well-defined $\pi \rightarrow \pi^*$ electronic transitions in the Q-band region near 560 nm ($a_{2u} \rightarrow e_g$) and the B-band region near 410 nm ($a_{1u} \rightarrow e_g$)[13] are replaced by a spectrum that arises from a series of overlapping bands.[4] The unpaired electron in the π-cation-radical species that are formed by one-electron oxidation of the porphyrin ring may reside in either the a_{1u} or the a_{2u} orbital, resulting in either $^2A_{1u}$ (commonly observed for phthalocyanines) or $^2A_{2u}$ (commonly observed for metallotetraphenylporphyrins) ground states.[15,16] The overall shape of the spectral envelope in the UV-visible region has served for a long time as the most well-used, discriminating criterion for determining which of the two possible electronic ground states of the π-cation-radical species is present. MCD spectra provide a much more detailed criterion.

Reversing the order of the top filled MO's, ($a_{1u}^2a_{2u}^1$) vs ($a_{2u}^2a_{1u}^1$), when the π cation radical forms is expected to result in drastic changes in the configuration interaction that links the Q- and B-band intensities in porphyrins where the a_{2u} orbital lies above, or accidently degenerate with, the a_{1u} orbital.[13] Despite the many absorption spectra published for porphyrin π-cation-radical complexes, the absorptions have not yet been systematically characterized.

For $[Co^{III}OEP(-1)]^{\bullet 2+}$, two different π-cation-radical species have been characterized on the basis of optical absorption and ESR spectral evidence[15,16] as being typical representatives of these two ground states. $[Co^{III}OEP(-1)]^{\bullet 2+}(Br^-)_2$ is associated with the $^2A_{1u}$ ground state, and $[Co^{III}OEP(-1)]^{\bullet 2+}(ClO_4^-)_2$, with the $^2A_{2u}$ ground state. The spectral properties of these two radical species have also been used as models for the redox chemistry of peroxidase enzymes due to a striking similarity between their optical absorption and MCD spectra and those of catalase compound I and HRP compound I.[8,17,18]

A number of methods have been applied to the identification of the ground state in porphyrin π-cation-radical species. We have described[4] MCD spectral patterns for the $^2A_{1u}$ and $^2A_{2u}$ ground states. An infrared band at 1280 cm^{-1} that is diagnostic for the porphyrin π cation radical has been identified.[19] Analysis of

* To whom correspondence should be addressed.
† Current address: Department of Chemistry, University of Virginia, Charlottesville, VA.

(1) Fuhrhop, J.-H.; Mauzerall, D. J. *J. Am. Chem. Soc.* **1969**, 91, 4174.
(2) Wolberg, A.; Manassen, J. *J. Am. Chem. Soc.* **1970**, *92*, 2982.
(3) Fajer, J.; Borg, D. C.; Forman, A.; Dolphin, D.; Felton, R. H. *J. Am. Chem. Soc.* **1970**, *92*, 3451.
(4) Browett, W. R.; Stillman, M. J. *Inorg. Chim. Acta* **1981**, *49*, 69.
(5) Nyokong, T.; Gasyna, Z.; Stillman, M. J. *Inorg. Chem.* **1987**, *26*, 1087.
(6) Stillman, M. J.; Nyokong, T. In *Phthalocyanines. Principles and Properties*; Lever, A. B. P., Leznoff, C. C., Eds.; VCH Publications: New York, 1989; pp 133-289.
(7) We will adopt the nomenclature used for phthalocyanine complexes[6] to describe the oxidation state of the porphyrin ring. In this nomenclature, the dianion of the porphyrin ring is written as OEP(-2); when the dianion is complexed with M(II), a neutral species is formed. A ring-oxidized complex is written as OEP(-1) and further defined by including the radical charge, as in $[Co^{II}OEP(-1)]^{\bullet+}$.
(8) Dolphin, D.; Forman, A.; Borg, D. C.; Fajer, J.; Felton, R. H. *Proc. Natl. Acad. Sci. U.S.A.* **1971**, *68*, 614.
(9) Felton, R. H.; Dolphin, D.; Borg, D. C.; Fajer, J. *J. Am. Chem. Soc.* **1969**, *91*, 196.
(10) Datta-Gupta, N. *Inorg. Chem.* **1971**, *33*, 4219.
(11) Salehi, A.; Oertling, W. A.; Babcock, G. T.; Chang, C. K. *J. Am. Chem. Soc.* **1986**, *108*, 5630.
(12) Nyokong, T.; Gasyna, Z.; Stillman, M. J. *Inorg. Chem.* **1987**, *26*, 548.
(13) (a) Gouterman, J. *J. Chem. Phys.* **1959**, *30*, 1139. (b) Gouterman, M. *J. Mol. Spectrosc.* **1961**, *6*, 138.
(14) (a) Barth, G.; Linder, R. E.; Bunnenberg, E.; Djerassi, C.; Seamans, L.; Moscowitz, A. *J. Chem. Soc., Perkin Trans. II* **1974**, 1706. (b) Stillman, M. J.; Thomson, A. J. *J. Chem. Soc., Faraday Trans. II* **1974**, *70*, 805.
(15) Fajer, J.; Borg, D. C.; Forman, A.; Felton, R. H.; Vegh, L.; Dolphin, D. *Ann. N. Y. Acad. Sci.* **1973**, *206*, 349.
(16) Fajer, J.; Davis, M. S. In *Porphyrins*; Dolphin, D., Ed., Ed.; Academic Press: New York, 1979, Vol. 4, p 197.
(17) Browett, W. R.; Stillman, M. J. *Biochem. Biophys. Acta* **1980**, *623*, 21.
(18) Browett, W R.; Stillman, M. J. *Biochem. Biophys. Acta* **1981**, *660*, 1.
(19) Shimomura, E. T.; Phillippi, M. A.; Goff, H. M.; Scholz, W. F.; Reed, C. A. *J. Am. Chem. Soc.* **1981**, *103*, 6778.

0020-1669/90/1329-5101$02.50/0

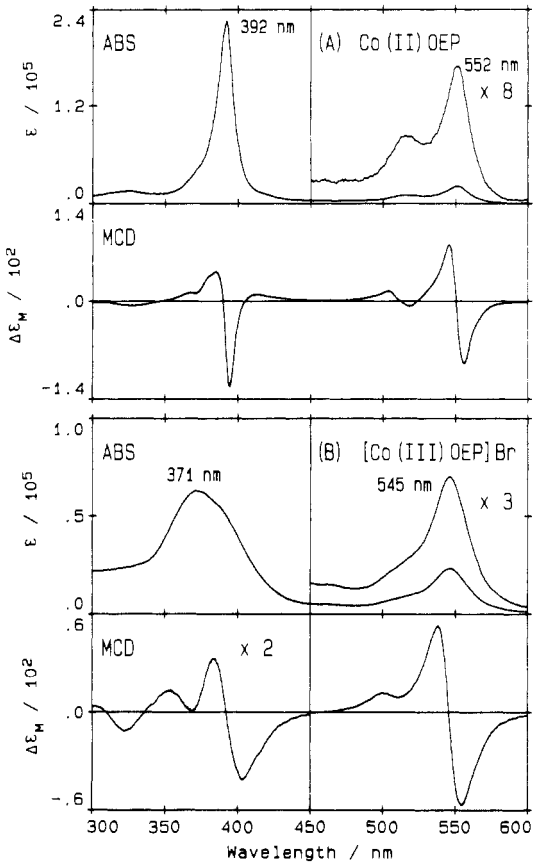

Figure 1. Absorption and MCD spectra of (A) $Co^{II}OEP(-2)$ in CH_2Cl_2 with absorption band maxima at 392 and 552 nm and (b) $[Co^{III}OEP(-2)]Br$ in CH_2Cl_2 with absorption band maxima at 371 and 545 nm.

NMR spectra[20] of $[Co^{III}OEP(-1)]^{\bullet 2+}(ClO_4^-)_2$ and $[Co^{III}OEP(-1)]^{\bullet 2+}(Br^-)_2$ radicals suggested that a thermal equilibrium exists between the $^2A_{1u}$ and $^2A_{2u}$ states, with the greater contribution being placed on the $^2A_{1u}$ state for $[Co^{III}OEP(-1)]^{\bullet 2+}(ClO_4^-)_2$ than for $[Co^{III}OEP(-1)]^{\bullet 2+}(Br^-)_2$. Analyses of resonance Raman spectra of the cobalt(III) octaethylporphyrin π cation radicals suggested a uniform $^2A_{1u}$ state for all OEP-based metallocomplexes,[21,22] although the significant differences in optical properties between different OEP π-cation-radical species was not addressed by these authors. A difference in reactivity pattern of these two radical species for reactions at the porphyrin ring[23] provides chemical evidence for the different distribution of the unpaired spin density in the two radicals. Finally, our study of the temperature dependence of the MCD spectrum of $[Co^{III}OEP(-1)]^{\bullet 2+}(ClO_4^-)_2$ and $[Co^{III}OEP(-1)]^{\bullet 2+}(Br^-)_2$ indicated significant differences in the coupling between the paramagnetic ring and Co(III), such that MCD C terms measured at near 4.2 K are quite different, which again suggests that the ground states in these two species are not the same.[24]

This lack of agreement between optical data, NMR data, and resonance Raman results represents a major problem in the assignment of electronic ground states of the porphyrin π-cation-radical species.

In this work, absorption and MCD spectral properties of a number of $[Co^{III}OEP(-2)]X$, $[Co^{II}OEP(-1)]^{\bullet +}X^-$, and $[Co^{III}OEP(-1)]^{\bullet 2+}(X^-)_2$ complexes are reported and compared with data for MgOEP(−1) and ZnTPP(−1), in order to examine the effect of the ground state on the optical spectrum. The effect of the counterion Cl^-, Br^-, ClO_4^-, or $SbCl_6^-$ in the stabilization of the site of oxidation is discussed.

Experimental Section

Materials and Methods. Cobalt(II) octaethylporphyrin ($Co^{II}OEP(-2)$, Aldrich) was dissolved in purified CH_2Cl_2 (BDH Chemicals). Oxidation at room temperature was carried out by using a number of oxidants: (1) Br_2 dissolved in CCl_4, (2) tris(*p*-bromophenyl)ammonium hexachloroantimonate in CH_2Cl_2, (3) solid $AgClO_4$, and (4) $FeCl_3$ dissolved in CH_2Cl_2. Photooxidation was carried out in CH_2Cl_2 solutions that contained 20% (v/v) CCl_4, as described previously.[25,26] Bromide to perchlorate ligand exchange was achieved by passing the solution over solid $AgClO_4$.

Absorption (CARY Model 219) and MCD spectra (JASCO Model J-500C spectrometer controlled by an IBM Instruments S9001 computer using the program CDSCAN5[27]) were recorded digitally. MCD spectra were recorded at 5.5 T (Oxford Instruments SM2 superconducting magnet) at room temperature, and the field strength and sign were calibrated by using the visible-region band of aqueous $CoSO_4$ ($\Delta\epsilon_M = -1.9 \times 10^{-2}$ L mol^{-1} cm^{-1} T^{-1} at 510 nm).

Calculations. The magnetooptical properties of the $Co^{II}OEP(-2)$ and $[Co^{III}OEP(-2)]X$ complexes, where $X^- = Cl^-$, Br^-, or $SbCl_6^-$, were characterized with expressions outlined by Ceulemans et al.[25] that were based on Gouterman's "four-orbital" model for the D_{4h} porphyrin system.[13] The important parameters are as follows.

(i) The center of gravity, A_{1g}', of the first two allowed excitations, $a_{2u} \rightarrow e_g$ and $a_{1u} \rightarrow e_g$, which give rise to the Q and B bands, respectively, is defined by[26]

$$A_{1g}' = [E(a_{2u} \rightarrow e_g) + E(a_{1u} \rightarrow e_g)]/2 \quad (1)$$

(ii) The transition-moment lengths in the porphyrin plane for zeroth- and first-order biconfigurational transitions are defined as[28]

$$\langle B_k^0|k|G\rangle = R$$

$$\langle Q_k^0|k|G\rangle = r$$

$$\langle B_k^1|k|G\rangle = R\cos\nu + r\sin\nu$$

$$\langle Q_k^1|k|G\rangle = -R\sin\nu + r\cos\nu \quad (2)$$

where k is x or y, R and r are the transition parameters, and ν is a mixing coefficient.

(iii) The angular momenta of the excited states, L_B and L_Q, are defined from[29]

$$\langle B_\pm^0|l_z|B_\pm^0\rangle = \pm L_B \quad (3)$$

$$\langle Q_\pm^0|l_z|Q_\pm^0\rangle = \pm L_Q \quad (4)$$

$$\langle B_\pm^1|l_z|B_\pm^1\rangle = \pm L_B\cos^2\nu \pm L_Q\sin^2\nu \quad (5)$$

$$\langle Q_\pm^1|l_z|Q_\pm^1\rangle = \pm L_B\sin^2\nu \pm L_Q\cos^2\nu \quad (6)$$

A_{1g}' was calculated directly from the absorption spectrum. The ratio of the dipole strengths of the B and Q bands, $D_0(B)$ and $D_0(Q)$, expressed as a function of ν and ω, is[29]

$$D_0(Q)/D_0(B) = \tan^2(\nu - \omega) \quad (7)$$

with ω defined by $\tan\omega = r/R$. The following relationships were tested in the analysis to compare the values of $(R^2 + r^2)$ and $(L_Q + L_B)$ for this series of porphyrin complexes:

$$D_0(B) + D_0(Q) = 2e^2(R^2 + r^2)/3 \quad (8)$$

$$(A_1/D_0)(B) + (A_1/D_0)(Q) = L_Q + L_B \quad (9)$$

where $(A_1/D_0)(Q)$ and $(A_1/D_0)(B)$ are the Faraday A-term parameters

(20) Morishima, I.; Takamuki, Y.; Shiro, Y. *J. Am. Chem. Soc.* **1984**, *106*, 7666.
(21) Oertling, W. A.; Salehi, A.; Chang, C. K.; Babcock, G. T. *J. Phys. Chem.* **1989**, *93*, 1311.
(22) Czernuszewicz, R. S.; Macor, K. A.; Li, X.-Y.; Kincaid, J. R.; Spiro, T. G. *J. Am. Chem. Soc.* **1989**, *111*, 3860.
(23) Setsune, J.-I.; Ikeda, M.; Kishimoto, Y.; Kitao, T. *J. Am. Chem. Soc.* **1986**, *108*, 1309.
(24) Gasyna, Z.; Browett, W. R.; Stillman, M. J. *Inorg. Chem.* **1988**, *27*, 4619.
(25) Gasyna, Z.; Browett, W. R.; Stillman, M. J. *Inorg. Chem.* **1984**, *23*, 382.
(26) Gasyna, Z.; Browett, W. R.; Stillman, M. J. *Inorg. Chem.* **1984**, 24, 2440.
(27) Gasyna, Z.; Browett, W. R.; Nyokong, T.; Kitchenham, R.; Stillman, M. J. *Chemom. Intell. Lab. Sys.* **1989**, *5*, 233.
(28) Shelnutt, J. A.; Ortiz, V. *J. Phys. Chem.* **1985**, *89*, 4733.
(29) Ceulemans, A.; Oldenhof, W.; Gorller-Walrand, C.; Vanquickenborne, L. G. *J. Am. Chem. Soc.* **1986**, *108*, 1155.

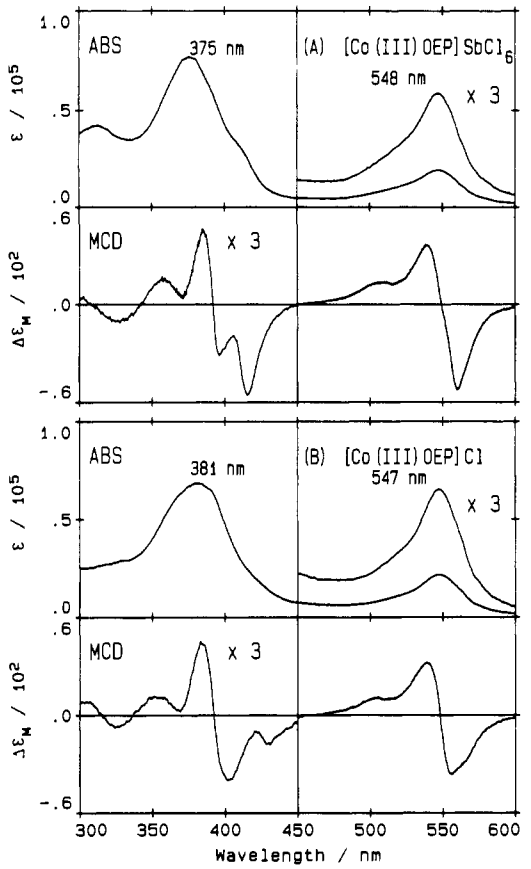

Figure 2. Absorption and MCD spectra of (A) $[Co^{III}OEP(-2)]SbCl_6$ in CH_2Cl_2 with absorption band maxima at 375 and 548 nm and (B) $[Co^{III}OEP(-2)]Cl$ in CH_2Cl_2 with absorption band maxima at 381 and 547 nm.

for the Q and B bands, respectively. The values of these parameters were calculated directly from the MCD spectra.

MCD expressions taken from Schatz and co-workers were used.[30] Both absorption and MCD spectra were fitted with Gaussian-shaped bands by using the program SIMPFIT.[31] The moments analysis was carried out by direct integration of the digitized absorption and MCD spectra. Spectra Manager was employed for the spectral data manipulation, analysis, and plotting.[32]

Results

Neutral $Co^{II}OEP$ and One-Electron, Metal-Oxidized $Co^{III}OEP$. Figure 1A shows the absorption and MCD spectra of neutral $Co^{II}OEP(-2)$. The presence of positive *A* terms[30] is indicative of degeneracy in the π^* excited states. The asymmetric MCD envelope under the B-band envelope (at 392 nm) and the low-energy shoulder near 420 nm are evidence that charge-transfer transitions also lie in this region. Figures 1B and 2A,B show the absorption and MCD spectra for a series of one-electron, metal-oxidized species: $[Co^{III}OEP(-2)]Br$, $[Co^{III}OEP(-2)]SbCl_6$, and $[Co^{III}OEP(-2)]Cl$, respectively.

Similar band patterns in the spectra of these compounds, with B and Q bands located at the normal positions of Co(III) derivatives, that is near 380 nm for the B band and near 547 nm for the Q band (Table I), support the assignment of metal oxidation. For each of the main absorption bands in the oxidized species (Figures 1B and 2A,B) there exists a similar MCD band that is characteristic of the $\pi \rightarrow \pi^*$ transition of an unoxidized porphyrin ring. The visible-region MCD spectrum exhibits a symmetric, derivative-type signal indicative of the underlying MCD *A* term. The pattern of high Q-band MCD intensity vs low B-band MCD intensity is that expected for diamagnetic d^6 porphyrin complexes. Significantly, the MCD spectra show that

Table I. Theoretical Band Energies and Oscillator Strengths (in Parentheses) of Cobalt(III) Porphyrin[35] Compared with the Observed Band Positions and Intensities and Calculated Band Energies and Oscillator Strengths Found by the Deconvolution of the Absorption and MCD Spectra of $[Co^{III}OEP(-2)]Br$

		theory[c]	
obsd[a] energy (1000 cm^{-1}, λ)	calcd[b] energy (osc)	transition	energy (osc)
		$^1E_g(d_\pi \rightarrow d_{z^2})$	12.4
		$^1A_{1u}(a_{1u} \rightarrow d_{z^2})$	14.4
	17.6 (0.02)	$^1A_{2u}(a_{2u} \rightarrow d_{z^2})$	16.1 (0.02)
18.2 (m) (Q_{00}, 550 nm)	18.3 (0.08) (*A*)	$^1E_u(\pi - \pi^*)$ (Q_{00})	17.3 (0.12)
	18.8 (0.01)		
	19.1 (0.03)		
20.0 (w) (Q_{01}, 500 nm)	19.7 (0.02) (*A*)		
	20.5 (0.01)	$^1B_{1u}(a_{1u} \rightarrow d_{x^2-y^2})$	21.2
	21.0 (0.01)	$^1B_{2u}(a_{2u} \rightarrow d_{x^2-y^2})$	23.0
	22.5 (0.03)	$^1B_{2g}(d_{xy} \rightarrow d_{z^2})$	23.9
	23.7 (0.06)	$^1E_g(d_\pi \rightarrow d_{x^2-y^2})$	24.9
	24.5 (0.05)		
27.0 (s) (B, 370 nm)	25.5 (0.30) (*A*)	$^1E_u(\pi - \pi^*)$ (B_{00})	29.5 (4.14)
	26.8 (0.33)	$^1A_{2g}(d_{xy} \rightarrow d_{x^2-y^2})$	31.3
	28.0 (0.34)		
	29.5 (0.10)		
	31.0 (0.22)		
	33.6 (0.30)		
		$^1E_u(\pi - \pi^*)$ (N)	37.8 (0.76)
		$^1A_{2u}(a_{2u} \rightarrow d_{z^2})$	37.8 (0.07)
		$^1E_u(\pi - \pi^*)$ (L)	40.4 (1.28)
		$^1E_u(\pi - \pi^*)$	44.8 (0.36)

[a] λ_{max} of the absorption spectrum based on the maxima in the spectral envelope. Band centers are given in units of 1000 cm^{-1} (nm). Intensity: (s) strong, (m) medium, and (w) weak; (sh) shoulder. [b] Calculated with band shape fitting programs to provide acceptable fits in both the absorption and the associated MCD spectra for $[Co^{III}OEP(-2)]Br$ in CH_2Cl_2. *A* indicates the presence of MCD *A* terms. [c] From ref 35 for cobalt(III) porphyrin.

the B-band transition is located on the red edge of the main absorption envelope and not at the band maximum (Table I). This is due to the presence of underlying charge-transfer transitions, as is also the case with phthalocyanine complexes.[33] $[Co^{III}OEP(-2)]Cl$ is selectively formed by irradiation of $Co^{II}OEP(-2)$, in CH_2Cl_2 containig CCl_4, with visible-region light directly into the Q band[25,26,34] according to the reactions

$$Co^{II}OEP(-2) \xrightarrow{h\nu} [Co^{II}OEP(-2)]^* \quad (10)$$

$$[Co^{II}OEP(-2)]^* + CCl_4 \rightarrow [Co^{III}OEP(-2)]Cl + \text{products} \quad (11)$$

The absorption and MCD spectra of the one-electron, metal-oxidized $[Co^{III}OEP(-2)]X$ compounds are considerably influenced by the counterion. We have attempted to quantify these differences by using the results of deconvolution analysis. It is important to note that the computer calculations were carried out on pairs of absorption and MCD spectra, in a fitting procedure that links individual bands in the absorption and MCD spectra.[31] The calcuations proceed until a single set of bands fits both absorption and MCD spectral envelopes satisfactorily.

From the analysis of $[Co^{III}OEP(-2)]Br$ (Figure 3), we identify major MCD *A* terms at 547 and at 392 nm, which are assigned to the Q_{00} and B transitions, respectively. The B band lies well to the red of the absorption band maximum. Table II shows (i) the energies of the band maxima determined directly from the spectra for the Q- and B-band regions, (ii) the energies and oscillator strengths obtained from the deconvolution calculations of the spectra, and (iii) theoretically predicted band energies and band assignments taken from Edwards and Zerner.[35]

Parameters for the Q and B transitions obtained from deconvolution calculations of the absorption and MCD spectra of $Co^{II}OEP(-2)$ and a series of $[Co^{III}OEP(-2)]X$ species (Table I)

(30) Piepho, S. B.; Schatz, P. N. In *Group Theory In Spectroscopy*; John Wiley and Sons: New York, 1983.
(31) Browett, W. R.; Stillman, M. J. *Comput. Chem.* **1987**, *11*, 241.
(32) Browett, W. R.; Stillman, M. J. *Comput. Chem.* **1987**, *11*, 73.
(33) Lever, A. B. P.; Licoccia, S.; Magnell, K.; Minor, P. C.; Ramaswamy, B. S. *ACS Symp. Ser.* **1982**, *No. 201*, 237.
(34) Gasyna, Z.; Browett, W. R.; Stillman, M. J. *Inorg. Chim. Acta* **1984**, *92*, 37.
(35) Edwards, W. D.; Zerner, M. C. *Can. J. Chem.* **1985**, *63*, 1763.

Table II. Fitting Parameters for the Q and B Bands of the Absorption and MCD Spectra of Neutral $Co^{II}OEP(-2)$ and Metal-Oxidized $[Co^{III}OEP(-2)]X$ Complexes in CH_2Cl_2

	Q_{00} band						
compd	ν^a	λ/nm	ϵ^b	$D_0/10^{4\,d}$	$B_0/10^{4\,d}$	A_1/D_0	μ^e
$Co^{II}OEP(-2)$	18 143	551	18 900	1.38	−54.4	2.50	2.34
$[Co^{III}OEP(-2)]Br$	18 281	547	21 400	3.11	−39.2	3.23	3.02
$[Co^{III}OEP(-2)]Cl$	18 128	552	20 100	3.22	−86.4	1.31	1.22
$[Co^{III}OEP(-2)]SbCl_6$	18 210	549	19 500	3.46	18.4	3.51	3.23
	Q_{01} band						
compd	ν^a	λ/nm	ϵ^b	D_0^c	$B_0/10^{4\,d}$	A_1/D_0	μ^e
$Co^{II}OEP(-2)$	19 433	516	9730	1.20	−10.56	1.12	1.05
$[Co^{III}OEP(-2)]Br$	19 674	508	5390	0.84	25.91	0.85	0.80
$[Co^{III}OEP(-2)]Cl$	19 674	508	5540	0.86	3.06	0.21	0.20
$Co^{III}OEP(-2)]SbCl_6$	19 674	508	6140	0.95	37.84	0.47	0.44
	B band						
compd	ν^a	λ/nm	ϵ^b	D_0^c	$B_0/10^{4\,d}$	A_1/D_0	μ^e
$Co^{II}OEP(-2)$	25 502	392	131 000	8.58	−126.6	0.32	0.30
$[Co^{III}OEP(-2)]Br$	25 487	392	42 600	8.46	5.1	1.09	1.02
$[Co^{III}OEP(-2)]Cl$	25 567	391	47 000	8.92	20.3	0.80	0.74
$[Co^{III}OEP(-2)]SbCl_6$	25 541	392	30 000	4.20	−2.0	0.95	0.89

[a] Calculated energy of the band maximum (cm^{-1}). [b] Calculated molar extinction coefficient (L mol^{-1} cm^{-1}). [c] D_0 is the calculated dipole strength in units of D^2. [d] The units of B_0 are D^2 cm. [e] μ = magnetic moment in units of Bohr magnetons, μ_B, calculated as $2 \times 0.4669 \times A_1/D_0$.[30]

show quantitatively the lack of systematic differences between the spectra of these species, with the exception of the greatly diminished B-band extinction coefficient of the Co(III) complexes (131 000 vs ca. 40 000). This is mainly because the B-band envelope is shared by at least three components in the Co(III) complexes, with the MCD *A* term located under the lowest energy band.

$Co^{II}OEP$ and $Co^{III}OEP$ complexes exhibit sufficiently well-resolved Q bands that a moments analysis based on numerical integration could be carried out through integration over the whole Q-band envelope (Table III). Strikingly, even though the B-band regions are quite different, the Q-band parameters are similar for both Co(II) and Co(III) complexes. Angular momentum ($2A/D$) values for the Q band of ca. 5.0 are approximately the same as reported previously for octaethylporphyrins and phthalocyanines.[14]

Table IV lists the model parameters for $Co^{II}OEP(-2)$ and a series of $[Co^{III}OEP(-2)]X$ complexes, generated by using eqs 1–9, together with the results from the computer deconvolution of the corresponding absorption and MCD spectra.

One-Electron Oxidation of $Co^{II}OEP$. Ring-Oxidized $Co^{II}OEP(-1)$. Figure 4 shows absorption and MCD spectra of $[Co^{II}OEP(-1)]^{\bullet+}ClO_4^-$ obtained when $Co^{II}OEP(-2)$ reacts with solid, anhydrous $AgClO_4$ in dry CH_2Cl_2. The sharp *A* term at 560 nm (asterisk) represents a very low fraction of neutral compound. A spectroscopically similar species is also formed by oxidation of $Co^{II}OEP(-2)$ with $FeCl_3$ in CH_2Cl_2 (Figure 5A). These reaction products clearly involve ring-centered oxidation to form π-cation-radical species. The characteristic visible-region MCD spectral features of a broad negative band centered on 600 nm and an overlapping series of positive bands between 420 and 550 nm have been observed to differing extents for all porphyrin π-cation-radical species for which MCD data are available, including the peroxidase and catalase compound I species.[17,18,47] Assignment of Co(II) to these two species is based on the lack

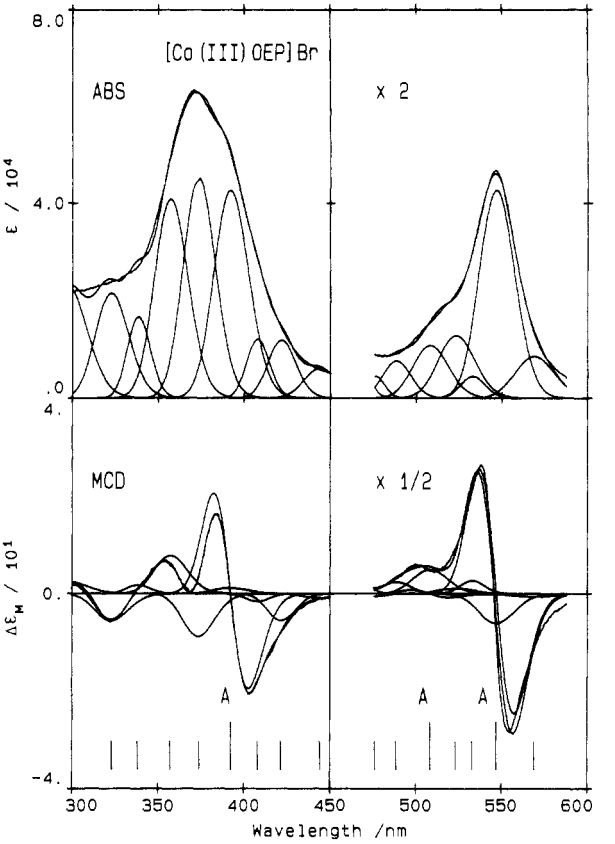

Figure 3. Results from a coupled-band analysis of the absorption and MCD spectra of $[Co^{III}OEP(-2)]Br$ in CH_2Cl_2. The A terms are derivative-shaped bands. The vertical bars mark the band centers of A and B terms. (Note: the experimental and fitted curves essentially overlap completely.)

of perturbation to the well-resolved *B* absorption and MCD *A* term, together with the significantly blue-shifted visible-region bands. The absorption and MCD spectra of neither of the species formed with perchlorate or $FeCl_3$ resemble the spectral data of the metal- and ring-oxidized complexes. Thus, the species obtained by oxidation with $AgClO_4$ can be described as $[Co^{II}OEP(-1)]^{\bullet+}ClO_4^-$. Identification of the counterion in the species obtained by the reaction of $Co^{II}OEP(-2)$ with $FeCl_3$ is difficult. The presence of Cl^- as the counterion in this complex can be excluded because the one-electron-oxidized species with a Cl^- counterion exhibit spectra similar to those of the Br^- compound, as shown in Figure 2B.

However, the MCD spectrum is unambiguous in the assignment of the oxidation site being the ring following reaction with $FeCl_3$ and perchlorate. The very broad, sweeping MCD signature in the visible region of both of these complexes is clearly due to ring oxidation from the a_{2u} HOMO (Figures 5 and 6) rather than the a_{1u} HOMO.

Two-Electron Oxidation of $Co^{II}OEP$. $Co^{III}OEP(-1)$ Species. Figure 6 shows the optical absorption and MCD spectra of the two-electron oxidation products of $Co^{II}OEP(-2)$, $[Co^{III}OEP(-1)]^{\bullet 2+}(Br^-)_2$, $[Co^{III}OEP(-1)]^{\bullet 2+}(ClO_4^-)_2$, and $[Co^{III}OEP(-1)]^{\bullet 2+}(SbCl_6^-)_2$. Irradiation of $Co^{II}OEP(-2)$ in CH_2Cl_2 containing CCl_4 with broad-band visible light formed a product with absorption and MCD spectra that closely resembled those of $[Co^{III}OEP(-1)]^{\bullet 2+}(Br^-)_2$. We ascribe these spectra to

Table III. Moment Analysis of the Q-Band Absorption and MCD Spectra of Neutral $Co^{II}OEP(-2)$ and Metal-Oxidized $[Co^{III}OEP(-2)]X$ Complexes in CH_2Cl_2

complex	ν/cm^{-1}	D_0	$\langle\Delta\epsilon_M\rangle_1$	A_1^a	A_1/D_0	$\langle\Delta\epsilon_M\rangle_0$	$B_0/10^{-3}$	$B_0/D_0/10^{-4}$
$Co^{II}OEP(-2)$	18 775	5.3	1950	12.8	2.41	0.11	0.74	1.40
$[Co^{III}OEP(-2)]Br$	18 665	6.6	2800	18.4	2.77	0.34	2.22	3.35
$[Co^{III}OEP(-2)]Cl$	18 664	7.4	2410	15.8	2.14	0.52	3.41	4.61
$[Co^{III}OEP(-2)]SbCl_6$	18 770	7.0	2960	19.4	2.77	0.04	0.29	0.41

[a] A_1 has units of D^2. Other parameters are defined as in Table II.

Table IV. Model Parameters for Neutral ZnOEP, $Co^{II}OEP(-2)$, and Metal-Oxidized $[Co^{III}OEP(-2)]x$ Series

complex	A_{1g}/cm^{-1}	$R^2 + r^2/Å^2$	$L_Q + L_B/\hbar$	$\lvert\nu - \omega\rvert$/ deg
$Zn^{II}OEP^a$	21 190	2.3	5.21	14.7
$Co^{II}OEP(-2)$	21 834	0.64	2.82	21.8
$[Co^{III}OEP(-2)]Br$	21 884	0.70	4.72	30.6
$[Co^{III}OEP(-2)]Cl$	21 847	0.75	4.14	28.5
$[Co^{III}OEP(-2)]SbCl_6$	21 875	0.45	6.32	38.9

[a] Data from ref 29.

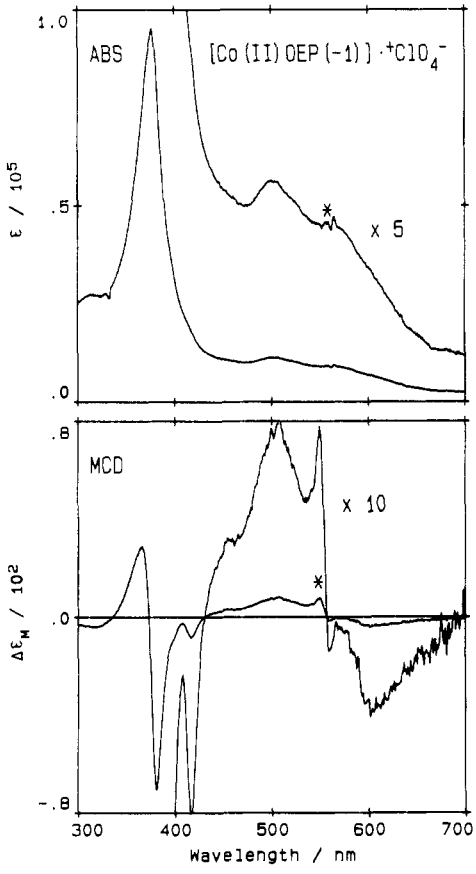

Figure 4. Absorption and MCD spectra of $[Co^{II}OEP(-1)]^{\bullet+}ClO_4^-$ formed by oxidation of $Co^{II}OEP(-2)$ with $AgClO_4$ in CH_2Cl_2. The asterisk indicates a band due to residual neutral porphyrin.

$[Co^{III}OEP(-1)]^{\bullet 2+}(Cl^-)_2$, which is formed according to reactions 12 and 13, which follow reactions 10 and 11. Reaction 13 does not go cleanly to completion.

$$[Co^{III}OEP(-2)]Cl \xrightarrow{h\nu} \{[Co^{III}OEP(-2)]Cl\}^* \quad (12)$$

$$\{[Co^{III}OEP(-2)]Cl\}^* + CCl_4 \rightarrow [Co^{III}OEP(-1)]^{\bullet 2+}(Cl^-)_2 + \text{products} \quad (13)$$

It is striking from Figure 6 that the $[Co^{III}OEP(-1)]^{\bullet 2+}$ species coordinated by ClO_4^- and $SbCl_6^-$ exhibit MCD spectra that are almost identical, whereas the spectrum of the Br^- complex is quite different, especially with respect to the intensity distribution between 550 and 700 nm.

Figures 7–9 show results of the deconvolution of the absorption and MCD spectra of $[Co^{III}OEP(-1)]^{\bullet 2+}(Br^-)_2$ and $[Co^{III}OEP(-1)]^{\bullet 2+}(ClO_4^-)_2$, respectively. The absorption and MCD spectra were fitted as pairs, with the same parameters in both spectra in order to reduce the obvious problems with ambiguity. Examples of this approach have been previously described.[6,31] For the better resolved spectra from the Br^- radical (Figure 7), we were able to calculate an acceptable fit on the basis of the *B* terms only, in which all major features are adequately accounted for by bands in both the absorption and MCD spectra. The fit of the B-band spectral data from the ClO_4^- complex (Figure 8) was more dif-

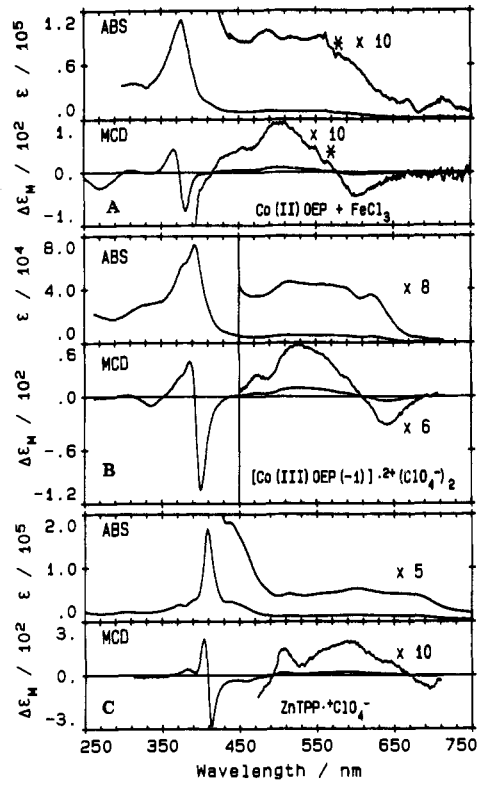

Figure 5. Absorption and MCD spectra of proposed $^2A_{2u}$ radical-cation species (A) $Co^{II}OEP(-1)$, formed from oxidation with $FeCl_3$, and (B) $Co^{II}OEP(-1)$ and (C) ZnTPP(-1), with ClO_4^- as a counterion. The asterisk in (A) indicates a band due to residual neutral porphyrin.

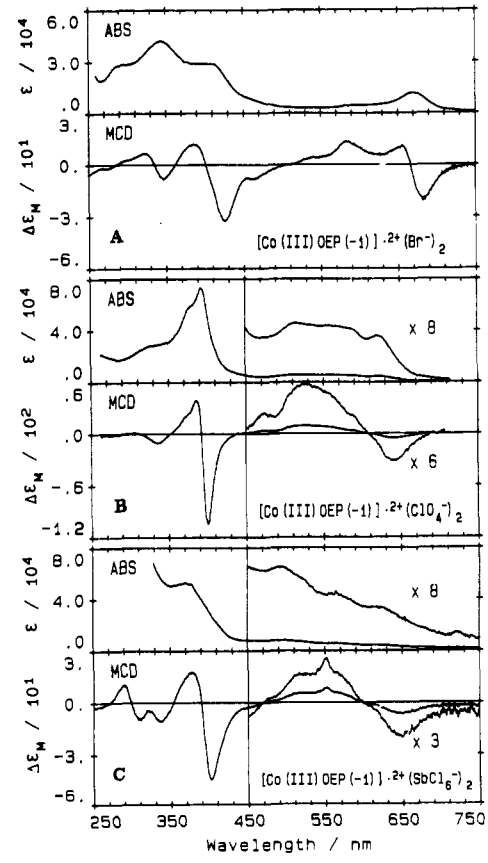

Figure 6. Absorption and MCD spectra of (A) $[Co^{III}OEP(-1)]^{\bullet 2+}(Br^-)_2$, formed by oxidation of $Co^{II}OEP(-2)$ with Br_2 in CH_2Cl_2, (B) $[Co^{III}OEP(-1)]^{\bullet 2+}(ClO_4^-)_2$, formed by exchange of Br^- by ClO_4^- in $[Co^{III}OEP(-1)]^{\bullet 2+}(Br^-)_2$ with $AgClO_4$ in CH_2Cl_2, and (C) $[Co^{III}OEP(-1)]^{\bullet 2+}(SbCl_6^-)_2$, formed by oxidation of $Co^{II}OEP(-2)$ with tris(*p*-bromophenyl)ammonium hexachloroantimonate in CH_2Cl_2. (A) and (B) were replotted from ref 24.

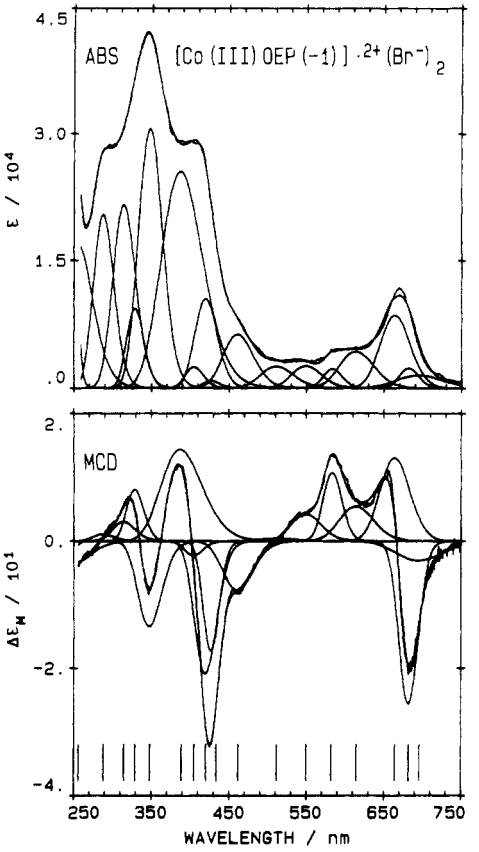

Figure 7. Results from a coupled-band analysis for the absorption and MCD spectra of $[Co^{III}OEP(-1)^{\cdot 2+}(Br^-)_2$ ($^2A_{1u}$) in CH_2Cl_2. Only B terms were used in the fit to the MCD spectrum.

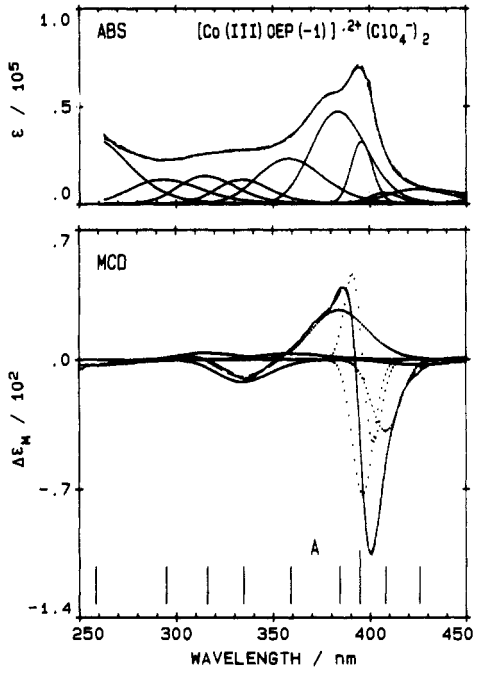

Figure 8. Results from a coupled-band analysis for the B-band region absorption and MCD spectra of $[Co^{III}OEP(-1)]^{\cdot 2+}(ClO_4^-)_2$ ($^2A_{2u}$) in CH_2Cl_2: (—) experimental data; (---) fitted data. A single A term (marked by the longer vertical bar) was used in the fit to the MCD spectrum.

ficult. The B-band-region MCD features extend over a very narrow energy range (we have split the data up for this reason); only a fit with an *A* term centered under the absorption band maximum (indicated by the longer dash in Figure 8) would fill both envelopes at all well. Tables V and VI list the fitting parameters obtained from the deconvolution calculations, together

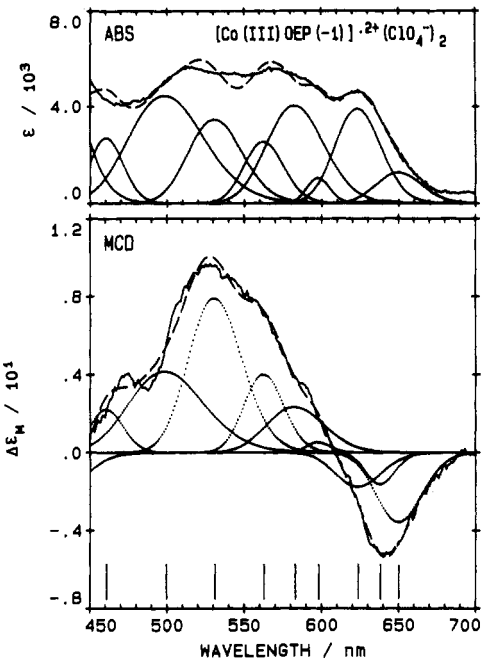

Figure 9. Results from a coupled-band analysis for the Q-band region absorption and MCD spectra of $[Co^{III}OEP(-1)]^{\cdot 2+}(ClO_4^-)_2$ ($^2A_{2u}$) in CH_2Cl_2: (—) experimental data; (---) fitted data; (···) individual MCD bands. Only B terms were used in the fit to the MCD spectrum.

Table V. Theoretical Band Energies and Oscillator Strengths (in Parentheses) of the $^2A_{1u}$ π-Cation-Radical Porphyrin[35] Compared with the Observed Band Positions and Intensities and Calculated Band Energies and Oscillator Strengths Found by the Deconvolution of the Absorption and MCD Spectra of the $^2A_{1u}$ π-Cation-Radical Species Metal- and Ring-Oxidized $[Co^{III}OEP(-1)^{\cdot 2+}(Br^-)_2$

excited-state sym[a]	theory[a] energy (osc)	obsd[b] λ/nm	obsd[b] energy (int)	calcd[c] energy (osc)
				14.4 (0.010)
				14.6 (0.007)
^2E_g	15.1 (0.095)	667	15.0 (m)	15.1 (0.040)
$^2A_{2g}$	17.3 (0.001)	602	16.6 (w)	16.3 (0.027)
^2E_g	18.1 (0.041)			17.1 (0.009)
$^2A_{2g}$	18.3 (0.015)	546	18.3 (w)	18.1 (0.018)
	18.6 (0.007)			19.5 (0.022)
				21.7 (0.062)
				23.4 (0.005)
^2E_g	19.5 (0.000)			23.8 (0.092)
				24.6 (0.019)
^2E_g	31.3 (1.908)	410	24.4 (m)	25.7 (0.483)
^2E_g	33.2 (0.209)			28.7 (0.419)
$^2A_{2g}$	37.6 (0.016)			30.4 (0.104)
^2E_g	37.7 (1.234)	340	29.4 (s)	31.8 (0.343)
$^2A_{2g}$	38.9 (0.042)			34.7 (0.348)
^2E_g	39.2 (0.805)	285	35.1 (s)	39.1 (0.519)
^2E_g	41.8 (0.021)			

[a] From ref 35. Band centers are given in units of 1000 cm^{-1}. [b] λ_{max} of the absorption spectrum. Intensity: (s) strong, (m) medium, and (w) weak; (sh) shoulder. [c] Calculated with band shape fitting programs to provide acceptable fits to both the absorption and the associated MCD spectra.

with theoretical values reported by Edwards and Zerner.[35]

Discussion

One-Electron Oxidation of $Co^{II}OEP$. Metal-Oxidized Species. One-electron oxidation can lead either to metal-oxidized or porphyrin-ring-oxidized species. Metal-oxidized $[Co^{III}OEP(-2)]X$ species are formed with Cl^-, Br^-, or $SbCl_6^-$. (An alternative structural assignment for these one-electron oxidation products is a mixed diaxial species, $[Co^{III}OEP(-2)](X)(Y)$, with a neutral second axial lignad Y, such as H_2O.) But, in either case, it is the metal that has been oxidized.

The visible and UV regions in the electronic spectra of many neutral metalloporphyrins have been successfully described in

Table VI. Theoretical Band Energies and Oscillator Strengths (in Parentheses) of the $^2A_{2u}$ π-Cation-Radical Porphyrin[35] Compared with the Observed Band Positions and Intensities and Calculated Band Energies and Oscillator Strengths Found by the Deconvolution of the Absorption and MCD Spectra of the $^2A_{2u}$ π-Cation-Radical Species Metal- and Ring-Oxidized $[Co^{III}OEP(-1)]^{\bullet 2+}(ClO_4^-)_2$

excited-state sym[a]	theory[a] energy (osc)	obsd[b] λ/nm	obsd[b] energy (int)	calcd[c] energy (osc)
				15.4 (0.005)
				15.7 (0.000)
^2E_g	14.7 (0.006)	640	15.7 (w)	16.0 (0.16)
^2E_g	15.5 (0.001)			16.7 (0.002)
	17.0 (0.039)			17.2 (0.024)
				17.8 (0.011)
$^2A_{1g}$	18.7 (0.009)	515	19.4 (m)	18.8 (0.023)
				20.0 (0.047)
				21.7 (0.015)
				23.5 (0.071)
^2E_g	19.5 (0.003)			24.5 (0.027)
^2E_g	28.1 (0.165)			25.2 (0.119)[d]
^2E_g	31.8 (3.252)	395	25.3 (s)	26.0 (0.488)
$^2A_{1g}$	34.9 (0.029)	375	26.7 (sh)	27.8 (0.320)
^2E_g	36.1 (0.021)			29.9 (0.161)
^2E_g	37.2 (0.075)	325	30.8 (w)	31.6 (0.224)
$^2A_{1g}$	39.6 (0.009)			33.9 (0.275)
^2E_g	40.8 (0.118)			

[a] From ref 35. Band centers are given in units of 1000 cm^{-1}. [b] λ_{max} of the absorption spectrum. Intensity: (s) strong, (m) medium, and (w) weak; (sh) shoulder. [c] Calculated with band shape fitting programs to provide acceptable fits to both the absorption and the associated MCD spectra. [d] Fit with an MCD *A* term.

terms of Gouterman's "four-orbital" model.[13,36,37] More recent calculations for cobalt(III) porphyrin[35] have shown that a number of charge-transfer bands span the optical spectrum. Some of these bands, especially those in the UV region, are predicted to have very low intensity. The effect of these bands might be to add in poorly resolved absorption that the fitting programs show as a band-shape mismatch.

The spectroscopic data for $Co^{II}OEP(-2)$ (Figure 1A) and $[Co^{III}OEP(-2)]X$ (Figures 1B and 2) show the effects of the mixing coefficient, v, and the transition moment length, r, the two different intensity-gaining mechanisms for the promotion of intensity in the Q band in D_{4h} porphyrins. Ceulemans et al.[29] used the framework of Gouterman's "four-orbital" model to interpret magnetooptical data for a series of axially substituted zinc porphyrin complexes. In this model, axial perturbation through ligand coordination by the central metal ion has an effect only on the energy of the a_{2u} HOMO. With σ-donor nucleophiles, this is due to interaction with the p_z-valence orbital on the metal. Axial perturbation has no influence on the a_{1u} HOMO, since this HOMO has nodes on the pyrrolic nitrogens. Increase in the σ-donor strength of the axial ligand leads to increasing destabilization of the a_{2u} HOMO. Increase in the a_{2u} orbital energy with strong axial ligands induces lowering of the transition-energy parameter A_{1g}'.[29] Among the parameters that determine the MCD expressions, only v depends on the a_{2u} orbital energy. The value of v will increase with an increase in the energy of the a_{2u} level. The values of the parameters defined by eqs 8 and 9 vary in the axial substitution series, which indicates that the axial ligand affects the optical transition characteristics in these complexes. Although comparison between our results and those of Ceuleman et al.[29] will need measurements of the spectra of a similar range of CoTPP complexes, the data do show that there are significant differences in coupling on changing from Zn(II) to Co(II) and Co(III). The reduction in $(L_Q + L_B)$ between Co(II) and Co(III) can be associated with the effects of overlapping charge-transfer transitions in the B-band region in $Co^{II}OEP$ (Figure 1).

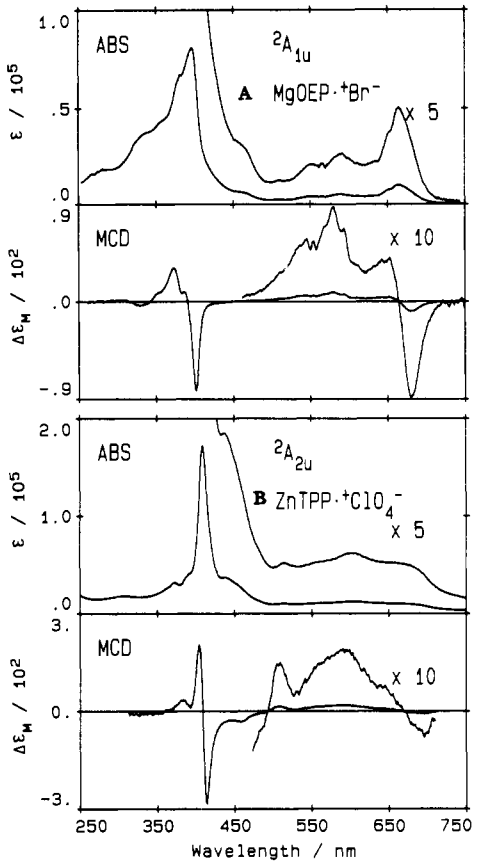

Figure 10. Absorption and MCD spectra of (A) $[MgOEP(-1)]^{\bullet+}Br^-$ ($^2A_{1u}$) and (B) $[ZnTPP(-1)]^{\bullet+}ClO_4^-$ ($^2A_{2u}$) in CH_2Cl_2.

We have shown,[25] on the basis of an analysis of MCD spectral data, that oxidation of CoTPP in CH_2Cl_2 results first in the metal-centered oxidation of Co(II) to Co(III). Similar results have been obtained[38] in recent FTIR studies of the electrochemical oxidation of CoTPP. It has also been suggested[39] that the one-electron oxidation product of CoTPP isolated with $SbCl_6^-$ as counterion is a $Co^{II}TPP(-1)$ π cation radical. As we have shown above, the site of oxidation in $Co^{II}OEP(-2)$ complexes is strongly dependent on the axial coordination. Absorption and MCD spectra of the $[Co^{III}OEP(-2)]X$ complexes, with X^- CL^-, Br^-, or $SbCl_6^-$, while similar enough to each other (Figures 1–3) are distinctively different from the spectra of $[Co^{II}OEP(-1)]^{\bullet+}ClO_4^-$ (Figure 4). Stabilization of either the metal or the ring as the specific oxidation site depends largely on the axial ligand. The presence of an axial ligand that coordinates more strongly than ClO_4^-, such as Br^-, results in oxidation of the metal. It is possible that the presence of an additional ligand in the $SbCl_6^-$ coordinated complex, such as water, also promotes the formation of the Co(III) species.

Although authenticated $[Co^{III}OEP(-2)]ClO_4$ has not yet been prepared to date,[11] our absorption and MCD data (Figure 1B) suggest strongly that Co(III) is present in the species with the $SbCl_6^-$ counterion (Figure 2A). These absorption and MCD spectra unequivocally indicate the absence of Co(II) in these $[Co^{III}OEP(-2)]X$ complexes due to the spectral pattern that is characteristic of diamagnetic d^6 porphyrin complexes (a broad, complicated B-band centered near 380 nm and a well-resolved Q-band MCD *A* term).

Presence of π Cation Radicals in Oxidized $Co^{II}OEP$. Oxidation of $Co^{II}OEP$ by $AgClO_4$ leads to the π-cation-radical species $[Co^{II}OEP(-1)]^{\bullet+}ClO_4^-$ (Figure 4). A similar $[Co^{II}OEP(-1)]^{\bullet+}X^-$ spectral structure is obtained by reaction with $FeCl_3$ (Figure 5A). Figure 5 compares the absorption and MCD spectra of

(36) Gouterman, M. In *The Porphyrins*; Dolphin, D., Ed.; Academic Press: New York, 1978; Vol. 3, Part A, p 1.
(37) McHugh, A. J.; Gouterman, M.; Weiss, C. *Theor. Chim. Acta* **1972**, *24*, 346.
(38) Hinman, A. S.; Pavelich, B. J.; McGarty, K. *Can. J. Chem.* **1988**, *66*, 1589.
(39) Scholtz, W. F.; Reed, C. A.; Lee, Y. J.; Scheidt, W. R.; Lang, G. *J. Am. Chem. Soc.* **1982**, *104*, 6791.

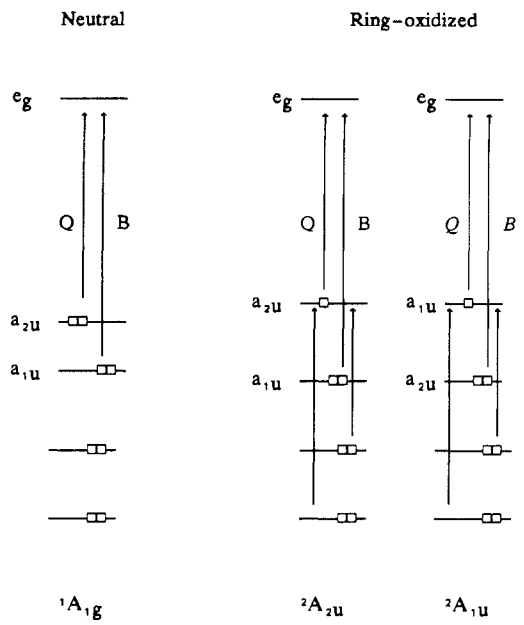

Figure 11. Electron distribution and optical transitions in neutral and ring-oxidized porphyrin complexes. Additional allowed transitions into the HOMO from low-lying filled MO's introduce strong new $\pi \rightarrow \pi$ absorptions in the visible–UV region of the spectrum. The terms "Q" and "B" refer to the first two singlet transitions in porphyrins and phthalocyanines, while both states transform as ^2E_u, the configuration interaction between the Q and B states that results in intensity borrowing for the lowest energy state, and a shift in transition energies[36] will be quite different for the $^2A_{2u}$ and $^2A_{1u}$ ground states. The scheme is based on Gouterman's four-orbital model.[36]

$[Co^{II}OEP(-1)]^{\bullet+}$, $[Co^{III}OEP(-1)]^{\bullet+}(ClO_4^-)_2$, and $[ZnTPP(-1)]^{\bullet+}$. All ring-oxidized porphyrin species for which the MCD spectra exhibit a characteristic sequence of MCD bands in the 500–700-nm region (Figures 5, 6, and 10). It is apparent from these MCD spectra that an almost identical signature is found in the visible region, red shifting from $Co^{II}OEP(-1)$ to $Zn^{II}TPP(-1)$. These spectral features are clearly not the same as those observed for MgOEP(−1) (Figure 10) or $[Co^{III}OEP(-1)]^{\bullet+}(Br^-)_2$ (Figure 6A), which we suggest is strong evidence that the $Co^{II}OEP(-1)$ species have a $^2A_{2u}$ ground state.

Spectral Characteristics of the π-Cation-Radical Species: $^2A_{1u}$ versus $^2A_{2u}$ Ground State. The absorption and MCD spectra in Figure 10 present the spectral patterns that are characteristic for the $^2A_{1u}$ and $^2A_{2u}$ ground states, on the basis of the well-established representatives of $MgOEP^{\bullet+}Br^-$ and $ZnTPP^{\bullet+}ClO_4^-$, respectively. The absorption spectral features used as indicators of molecular orbital involvement have been the resolution of the lowest energy band near 640 nm: well resolved for the $^2A_{1u}$ complexes and poorly resolved for the $^2A_{2u}$ complexes. The MCD spectrum adds far more information. The B-band region, traditionally, in the terms of Gouterman's 4-orbital model,[36] arises from allowed transitions out of the a_{1u} molecular orbital (Figure 11). We expect that the effect of the reversal in the order of the orbitals in order for the $^2A_{1u}$ ground state to form will drastically change the configuration interaction, which will change the orbital composition of the "B"-band excited state. We do not find it unexpected that the "B"-band region in MgOEP(−1) *and* $[Co^{III}OEP(-1)](Br)_2$, both $^2A_{1u}$, should exhibit similar MCD spectral features, because we find that $^2A_{2u}$ cation-radical complexes exhibit remarkably similar MCD spectra that are independent of metal (Figure 5). The spectra of the two classes of cation radical are quite different when compared together (Figure 10).

Characterization of the molecular orbitals involved in ring oxidation in metalloporphyrin π-cation radicals, $MP^{\bullet+}$, has been based on EPR and ENDOR studies,[16,40-42] as well as on MO calculations.[43-45] EPR and ENDOR measurements have provided spin-density profiles that have established that there are differences in the electronic ground states ($^2A_{2u}$ or $^2A_{1u}$). For diamagnetic species, such as the spin-coupled metalloporphyrin π cation radicals, other techniques have to be used. Theoretical calculations[35] applied to the π cation radicals of metalloporphyrins have predicted that the main optical transitions should be substantially different in species with either the $^2A_{1u}$ or $^2A_{2u}$ ground state. The energies and intensities of the optical transitions for the π-cation-radical species can be obtained by a band-fitting analysis of the absorption and MCD spectra.[5,46,47] Analysis[46] carried out for HRP compound I and catalase compound I reveals a number of spectral features that were predicted by the theory.[35] Analysis of the absorption and MCD spectral properties of $[Co^{III}OEP(-1)]^{\bullet2+}(Br^-)_2$ and $[Co^{III}OEP(-1)]^{\bullet2+}(ClO_4^-)_2$ at temperatures between 4 and 298 K[47] indicates that the observed temperature dependence results from the spin–orbit coupling in the excited π–π^* states due to charge-transfer states. The room-temperature MCD spectra were not dominated by *C* terms, as is evident by similarities between the spectral data for species such as MgOEP(−1) (Figure 10) and $[Co^{III}OEP(-1)]^{\bullet2+}(Br^-)_2$ (Figure 6A). We have seen no indication of an equilibrium mixture between the two ground states in either complex.

Resonance Raman (RR) frequencies of the $[M^{II/III}OEP(-1)]^{\bullet+}ClO_4^-$ complexes, where M = Ni, Co, Cu, and Zn, are similar for all radicals.[48] The RR frequency shift patterns have been used to suggest that all OEP radicals are $^2A_{1u}$ in character. From EPR measurements the Co hyperfine coupling constant has been reported to be only 1.2 G for $[Co^{III}OEP(-1)]^{\bullet2+}(ClO_4^-)_2$, compared with 5.6–5.7 G for the $[Co^{III}TPP(-1)]^{\bullet2+}(ClO_4^-)_2$ species.[2] A large hyperfine constant is expected for an a_{2u} radical because of the concentration of spin density on the pyrrole N atoms, which can delocalize onto the metal. The much smaller value observed for $[Co^{III}OEP(-1)]^{\bullet2+}(ClO_4^-)_2$ was used to suggest that this species is mainly a_{1u} in character.

This discrepancy in the assignment of ground state extends[18] to radicals such as $[Cu^{II}OEP(-1)]^{\bullet+}$,[49] $[Co^{II}OEP(-1)]^{\bullet+}$ (this work, Figure 5), and $[Ni^{II}OEP(-1)]^{\bullet+}$, where analysis of the optical data imply $^2A_{2u}$ character for the ground state of the complexes with ClO_4^- ligands. The horseradish peroxidase compound I intermediate, which is a ferryl porphyrin cation radical, has been established[18,50] to be predominantly a_{2u} in character. Since the porphyrin in HRP is protoporphyrin IX, with the same substituent pattern as OEP, the radical would be expected to have a_{1u} character, and indeed this anomaly is explained in terms of strong axial ligands changing the ground state. The effects of the axial ligands are evidently sufficient to favor the a_{2u} character.

The origins of the optical transitions for the porphyrin system are schematically depicted in Figure 11. In neutral complexes of diamagnetic metals with the $^1A_{1g}$ ground state, the $a_{2u} \rightarrow e_g$ transition is responsible for the Q-band absorption near 560 nm and the $a_{1u} \rightarrow e_g$ transition gives rise to the B-band absorption found near 410 nm. As a result of the "accidental" degeneracy of the a_{1u} and a_{2u} MO's, a configuration interaction is significant, allowing intensity to be coupled from the "allowed" B band to the formally "forbidden" Q band. In the ring-oxidized species, the energies of the $a_{2u} \rightarrow e_g$ and the $a_{1u} \rightarrow e_g$ transitions will reflect the orbital ordering, which determines the ground state of the

(40) Fujita, E.; Chang, C. K.; Fajer, J. *J. Am. Chem. Soc.* **1985**, *107*, 7665.
(41) Chang, C. K.; Hanson, L. K.; Richardson, P. F.; Young, R.; Fajer, J. *Proc. Natl. Acad. Sci. U.S.A.* **1981**, *78*, 2652.
(42) Fujita, E.; Chang, C. K.; Fajer, J. *J. Am. Chem. Soc.* **1985**, *107*, 7665.
(43) Hanson, L. K.; Chang, C. K.; Davis, M. S.; Fajer, J. *J. Am. Chem. Soc.* **1981**, *103*, 663.
(44) Loew, G. H.; Herman, Z. S. *J. Am. Chem. Soc.* **1980**, *102*, 6174.
(45) Fujita, I.; Hanson, L. K.; Walker, F. A.; Fajer, J. *J. Am. Chem. Soc.* **1983**, *105*, 3296.
(46) Browett, W. R.; Gasyna, Z.; Stillman, M. J. *J. Am. Chem. Soc.* **1988**, *110*, 3633.
(47) Gasyna, Z.; Browett, W. R.; Stillman, M. J. *ACS Symp. Ser.* **1986**, *No. 321*, 298.
(48) Oertling, W. A.; Salehi, A.; Chung, Y. C.; Leroi, G. E.; Chang, C. K.; Babcock, G. T. *J. Phys. Chem.* **1987**, *91*, 5887.
(49) Godziela, G. M.; Goff, H. M. *J. Am. Chem. Soc.* **1986**, *108*, 2237.
(50) Roberts J. E.; Hoffman, B. M.; Rutter, R.; Hager, L. P. *J. Biol. Chem.* **1981**, *256*, 2118.

π-cation-radical species, i.e. $(a_{1u}{}^2a_{2u}{}^1)$ for the $^2A_{2u}$ state and $(a_{2u}{}^2a_{1u}{}^1)$ for the $^2A_{1u}$ state. The effect of the order of the top-filled MO's, $(a_{1u}{}^2a_{2u}{}^1)$ vs $(a_{2u}{}^2a_{1u}{}^1)$, on the excited states accessed under resonance conditions has not yet been examined as a possible source of the discrepancy in sensitivities between resonance Raman and optical spectral data. Additionally, while the resonance Raman spectra pick up the major differences in molecular structure between TPP and OEP ring systems, it is perhaps possible that the resonance Raman spectrum does not pick up changes as well within a single geometry.

In summary, MCD spectra discriminate between ground states in porphyrin π-cation-radical species possibly because the reversal of the a_{1u}/a_{2u} order significantly changes the orbitals within the excited states. The spectra in Figures 4, 5, and 6B,C correspond to the porphyrin complexes in which a_{2u} is the highest occupied MO for the π-cation-radical species. This type of spectrum is common for ZnTPP(-1) and Co(II)- and Co(III)-containing porphyrin π-cation radicals with ClO_4^- and $SbCl_6^-$ counterions. These a_{2u} π-cation-radical species exhibit a similar scrambling in the visible region but maintain an almost normal Soret region band that arises from the mostly unaffected $a_{1u} \rightarrow e_g$ transition.

The absorption and MCD spectra for MgOEP(-1) and $[Co^{III}OEP(-1)]^{\bullet 2+}(Br^-)_2$ shown in Figures 6A and 10A, respectively, are clearly not the same as the spectra recorded for ZnTPP(-1), our model for the $^2A_{2u}$ ground state. Some similarities exist between these spectral data and the resolved spectra observed for MgPc(-1) complexes[51] in which the ground state is clearly $^2A_{1u}$. The $^2A_{1u}$ species are characterized by the well-resolved lowest energy band first associated with the spectrum of catalase compound I.[8]

Acknowledgment. We wish to acknowledge financial support from the NSERC of Canada through Operating, Strategic and Equipment grants and the Academic Development Fund at the UWO for an equipment grant. We thank Dr. William R. Browett for his contribution to the early stages of this work. This is publication No. 433 of the Photochemical Unit at the UWO. We are associated with the Centre for Chemical Physics and the Photochemical Unit at the UWO.

(51) Ough, E.; Gasyna, Z.; Stillman, M. L. Submitted for publication in *Inorg. Chem.*

Contribution from the Departments of Biophysics and Chemistry, University of Rochester, Rochester, New York 14642, and The Squibb Institute for Medical Research, New Brunswick, New Jersey 08903-0191

Proton Magnetic Relaxation Dispersion in Aqueous Glycerol Solutions of $Gd(DTPA)^{2-}$ and $Gd(DOTA)^-$

Griselda Hernandez,[‡] Michael F. Tweedle,[§] and Robert G. Bryant*[,†,‡]

Received November 17, 1989

Nuclear magnetic relaxation rates are reported as a function of the magnetic field strength over the range of proton Larmor frequencies from 0.01 to 200 MHz for aqueous glycerol solutions of $Gd(DTPA)^{2-}$ and $Gd(DOTA)^-$ ions. The data are qualitatively described by the Solomon-Bloembergen-Morgan equations but are not described in detail by these equations. The effects of viscosity on the water proton relaxation efficiency are studied in particular to gain a better understanding of the dynamical factors controlling relaxation. The response of the nuclear relaxation to changes in the solution viscosity is a function of magnetic field strength because of compensating changes in the contributions of the rotational correlation times of the metal complexes and the electron spin-relaxation times to the effective correlation time for the electron-nuclear interaction.

Magnetic resonance imaging provides a safe and noninvasive imaging modality that is particularly useful for soft tissue discrimination. The basis for the contrast in the magnetic image is largely dominated by the differences in nuclear magnetic relaxation times among tissues.[1] Control of relaxation by spectroscopic or chemical means thus provides an additional diagnostic dimension that may be very useful in the identification of certain pathologies. Chelate complexes of gadolinium ion have been widely examined in this context because the high magnetic moment, labile coordinated water, and long electron spin-lattice relaxation times of this ion make these complexes generally efficient relaxation agents for the water proton spins in aqueous systems.[2,3] Currently, the most widely used complex is $Gd(DTPA)^{2-}$ (DTPA is diethylenetriaminepentaacetic acid);[4] however, other complexes such as $Gd(DOTA)^-$ (DOTA is 1,4,7,10-tetraazacyclododecane-1,4,7,10-tetraacetic acid) are more efficient in relaxing water proton spins. Both of these complexes are reported to provide one inner-sphere water molecule that exchanges rapidly with the solvent and couples the relaxation efficiency of the metal center to the whole solvent population.[5] Because these complexes are important representatives of a class of complexes, we report here nuclear magnetic relaxation dispersion measurements on highly purified materials as a function of the solution viscosity. This series of measurements displays the major features of the relaxation mechanisms operative in these complex ions and points to the important interplay between the electron spin-relaxation contribution to the correlation times for the electron-nuclear coupling and the rotational correlation time for the metal complex.

Experimental Section

Nuclear magnetic relaxation measurements were made on a field cycling spectrometer described elsewhere[6] that switches magnetic field strengths in real time from values limited by the earth's magnetic field to a proton Larmor frequency of 42 MHz. The relaxation rates were extracted from 16, 24, or 30 data points that were fitted to an exponential using a nonlinear least-squares procedure. The statistical errors were typically about 1%, though reproducibility was more nearly 5%. Samples were contained in 10-mm Pyrex sample tubes sealed with rubber stoppers and a screw cap. Temperature in the measurement coil was maintained by a flow of liquid perchloroethylene that was thermostated in an external Neslab RTE-8 temperature controller, which serviced the sample region by using outboard Little Giant pumps. Magnetic spin-lattice relaxation rates were also measured at a proton Larmor frequency of 200 MHz on a spectrometer described elsewhere.[7]

[†] Department of Biophysics, University of Rochester.
[‡] Department of Chemistry, University of Rochester.
[§] The Squibb Institute for Medical Research.

(1) Mansfield, P.; Morris, P. G. *NMR Imaging in Biomedicine*; Academic Press: New York, 1982.
(2) Koenig, S. H.; Brown, R. D., III. *Magn. Reson. Med.* **1984**, *1*, 478.
(3) Lauffer, R. B. *Chem. Rev.* **1987**, *87*, 901.
(4) Wainmann, H. J.; Brasch, R. C. *AJR, Am. J. Roentgenol.* **1984**, *142*, 619.
(5) Bryden, C. C.; Reilley, C. N. *Anal. Chem.* **1982**, *54*, 610.
(6) Hernandez, G.; Brittain, H. G.; Tweedle, M. F.; Bryant, R. G. *Inorg. Chem.* **1990**, *29*, 985.
(7) Jackson, C. L.; Bryant, R. G. *Biochemistry* **1989**, *28*, 5024.

0020-1669/90/1329-5109$02.50/0